ISSN 0030-400X, Optics and Spectroscopy, 2023, Vol. 131, No. 9, pp. 840–848. © Pleiades Publishing, Ltd., 2023.
Russian Text © The Author(s), 2022, published in Optika i Spektroskopiya, 2022, Vol. 130, No. 1, pp. 84–91.
English Text © Ioffe Institute, 2023.

Phase Diagram and Soft Modes Behavior $TbFe_{3-x}Ga_x(BO_3)_4$ Solid Solutions with Huntite Structure

A. S. Krylov[a,*], A. N. Vtyurin[a,b], I. A. Gudim[a], I. V. Nemtsev[a,b,c], and S. N. Krylova[a]

[a] *Kirensky Institute of Physics, Federal Research Center KSC SB, Russian Academy of Sciences, Krasnoyarsk, 660036 Russia*

[b] *Siberian Federal University, Krasnoyarsk, 660041 Russia*

[c] *Federal Research Center KSC SB, Russian Academy of Sciences, "Krasnoyarsk Scientific Center of the Siberian Branch of RAS," Krasnoyarsk, 660036 Russia*

**e-mail: shusy@iph.krasn.ru*

Received July 22, 2021; revised July 22, 2021; accepted August 7, 2021

Abstract—The Raman spectra of four crystals of $TbFe_{3-x}Ga_x(BO_3)_4$ solid solutions (x from 0 to 0.54) were studied in the temperature range from 8 to 350 K. The temperatures of structural phase transitions were determined. The observed spectral behavior is characteristic to condensation and restoration of soft modes. Soft modes are associated with a structural phase transition from the $R32$ phase to the $P3_121$ phase. The Compositions-Temperature phase diagram was constructed.

Keywords: Raman spectroscopy, temperature dependence, soft modes, ferroborates, phase diagramm

DOI: 10.1134/S0030400X23070081

INTRODUCTION

Rare-earth ferroborate crystals with the huntite structure [1] are promising materials for optoelectronic devices. For example, crystals with large values of the magnetoelectric effect [2] were found in this family. Such crystals can be used in mechanisms for controlling the electrical and magnetic properties of materials [3, 4]. The coexistence of magnetic and ferroelectric order parameters leads to the fact that crystals are multiferroics [5, 6]. The possibility of practical applications and the prospect of optimizing the characteristics by partial replacement of rare-earth ions or iron ions attract researchers [7–12]. In particular, the replacement of iron ion by gallium ion in $HoFe_3(BO_3)_4$ crystal leads to shift of the structural phase transition temperature [12].

The growth of crystals with the huntite structure and their primary characterization were previously presented in several papers [7, 8, 12]. These studies shown that the basic elements of $R32$ structure are helical chains of FeO_6 octahedrons directed along c axis. For the first time, in the paper [9] the phase transition from the structure $R32$ to $P3_121$ in terbium ferroborate was observed at 198 K. Note that the main study method in this paper was the method of Raman spectroscopy (RS). In subsequent studies of the crystal the phase transition temperature 192 K in $TbFe_3(BO_3)_4$ was determined by other methods [10, 14, 15].

The magnetic phase transition was discovered in $TbFe_3(BO_3)_4$ crystal at a temperature of about 40 K [12] and studied by various methods [10, 16–20]. It was found that the magnetic properties of crystal are determined by the interaction of two magnetic subsystems: the iron and terbium. At temperature T_N, an antiferromagnetic ordering of the iron subsystem occurs with magnetic moments directed along the three-fold axis C_3. At the same time, antiferromagnetic ordering caused by interaction with the iron subsystem also exists in the terbium subsystem with magnetic moments parallel to the same axis. Besides, a first-order spin-reorientation (magnetic) phase transition (H_c = 35 Oe at 4.2 K) [10, 14, 21] is induced in terbium ferroborate. D. Saller et al. [22] should be mentioned, in which the authors studied the magnetic resonances in $TbFe_3(BO_3)_4$ crystal. They supposed that there are six nonequivalent magnetic sublattices of Fe. For $TbFe_3(BO_3)_4$, $NdFe_3(BO_3)_4$, $NdGa_3(BO_3)_4$, $HoGa_3(BO_3)_4$ crystals also theoretical calculations based on the density functional theory [14, 15, 23, 24] were performed.

The region of low vibrational frequencies is the most interesting in the study of structural phase transitions, since the soft mode frequency tends to zero as the critical temperature is approached, which causes instability of the crystal structure. For the first time, a soft mode was observed in one of the representatives of the family of rare- earth ferroborates—in $GdFe_3(BO_3)$

Table 1. Composition of solution—melt (charge) in quasi-binary form and saturation temperature during synthesis of solid solutions of $TbFe_{3-x}Ga_x(BO_3)_4$

Composition of solution—melt (charge) in quasi-binary form: $(100-n)$ mass% $[Bi_2Mo_3O_{12} + pB_2O_3 + qTb_2O_3] + n$ mass% $TbFe_{3-x}Ga_x(BO_3)_4$						
Crystal	p	q	N	T_{sat}, °C	dT_{sat}/dn, °C/mass %	ΔT_{met}, °C
$TbFe_3(BO_3)_4$	2.5	0.5	26	960	4.5	≈12
$TbFe_{2.5}Ga_{0.5}(BO_3)_4$	2.5	0.5	27	948	4.0	
$TbFe_{2.45}Ga_{0.55}(BO_3)_4$	2.5	0.5	26	940	3.8	
$TbFe_{2.4}Ga_{0.6}(BO_3)_4$	2.5	0.5	26.7	960	3.8	

crystal [25]. Later, the methods of vibrational spectroscopy of light were repeatedly used to study structural and magnetic transitions in some ferroborates [13, 25–32]. The temperature studies of terbium were carried out in $TbFe_3(BO_3)_4$ crystal (without substitution of ions) by RS spectroscopy [9, 18, 33]. In this case, anomalies were observed in the low-frequency region of the vibrational spectra associated with the magnetic phase transition [9, 33], as well as anomalies in the medium- frequency region associated with the structural phase transition [18, 33]. It should be noted that soft modes in terbium ferroborate were observed not only in the RS spectra, but also in the infrared absorption spectra in M.N. Popova et al. [34].

It can be expected that with the temperature changes in $TbFe_{3-x}Ga_x(BO_3)_4$ solid solutions, the anomalies will be detected in the low-frequency region of RS spectra. The purpose of this work is to study the effect of the iron ions substitution by gallium ions in $TbFe_{3-x}Ga_x(BO_3)_4$ solid solutions on the temperature of structural phase transitions and the behavior of low-frequency spectral lines (soft modes).

The authors dedicate this article to Professor Marina Nikolaevna Popova on the occasion of her 80th birthday and for her great contribution to the study of ferroborates by optical spectroscopy methods [9, 20, 25, 34, 35].

EXPERIMENT

Single crystals $TbFe_3(BO_3)_4$, $TbFe_{2.5}Ga_{0.5}(BO_3)_4$, $TbFe_{2.45}Ga_{0.55}(BO_3)_4$ and $TbFe_{2.4}Ga_{0.6}(BO_3)_4$ (as per embedding) were grown from the solution-melt based on $(Bi_2Mo_3O_{12}–B_2O_3–Tb_2O_3)$ [36]. The corresponding compositions are presented in the Table 1.

Solution-melt with a weight of 150 g was prepared in a platinum cylindrical crucible (D = 40 mm, H = 50 mm) by sequential fusion of oxides Bi_2O_3, MoO_3, B_2O_3, Fe_2O_3, Ga_2O_3, Nd_2O_3 at 1100°C.

At the stage of dissolution at the same temperature the stirred solution-melt was kept for 8–10 h. This time is sufficient for its complete homogenization. The saturation temperature T_{sat} was determined with an accuracy of ±2°C using test crystals, which were previously obtained on a rod crystal holder in the spontaneous nucleation mode. After the final homogenization the temperature of the solution-melt was reduced to T_{sat} + 7°C, the rod with four seeds was immersed in the solution-melt, and its reverse rotation was started at a speed of 30 rpm. After 10 min the temperature was lowered to T_{sat} – 10° C and then was lowered smoothly according to the program with increasing rate dT/dt = 1–3°C/day. Growth continued from 5 to 14 days. During this time high-quality crystals grew with sizes up to 4–12 mm. The crystal holder with grown crystals was raised above the solution-melt, and the furnace cooled down to room temperature with the power turned off. Initially, $TbFe_3(BO_3)_4$ and $TbFe_{2.5}Ga_{0.5}(BO_3)_4$ crystals were synthesized; after studying the structural phase transitions in them a decision was made on additional synthesis of crystals with compositions $TbFe_{2.45}Ga_{0.55}(BO_3)_4$ and $TbFe_{2.4}Ga_{0.6}(BO_3)_4$. The time difference was several tens of months.

Raman spectra of the crystals were studied in the temperature range from 8 to 350 K. The spectra were obtained in backscattering geometry using a Horiba Jobin Yvon T64000 spectrometer (Horiba, France) with a triple monochromator operating in the subtraction dispersion mode. The spectral resolution for the recorded spectra of the Stokes component of the Raman spectrum was 2 cm^{-1} (this resolution was achieved using lattices with 1800lines/mm and 100 μm slits). The resolution of the low-frequency region in the study of the soft mode was improved to 1.2 cm^{-1}, which made it possible to reach the low-frequency limit of 10 cm^{-1}. As source of exciting light the lasers were used: Spectra-Physics Stabilite 2017 single-mode Ar^+ laser (USA) 514.5 nm and with power of 10 mW on sample ($TbFe_3(BO_3)_4$, $TbFe_{2.5}Ga_{0.5}(BO_3)_4$) and Spectra-Physics Excelsior-532-300-CDRH solid state single mode laser (USA) 532 nm and with power 5 mW on sample ($TbFe_{2.45}Ga_{0.55}(BO_3)_4$ and $TbFe_{2.4}Ga_{0.6}(BO_3)_4$). Temperature experiments were carried out in ARS CS204-X1.SS closed-cycle helium cryostat controlled by LakeShore 340 temperature

controller. The temperature was controlled by a calibrated silicon diode LakeShore DT-670SD1.4L. Indium foil was used as a thermal interface between the cold finger and the sample. The measurements were carried out in the cryostat previously evacuated to pressure of 10^{-6} mbar. During the temperature experiment the exciting beam performed a linear scanning over the sample surface with maximum amplitude of 0.3 mm. This made it possible, on the one hand, to average the effects caused by possible heating inhomogeneity, and, on the other hand, to reduce the heat load due to a more uniform distribution of the sample heating by the laser, and, as a result, decreasing of the temperature measurement error. The experiments were carried out in dynamic mode by varying the sample temperature. The temperature change rate was 0.8 K/min.

The uncertainty of the measured temperature for a given speed can be estimated as the difference between adjacent measurements. The total recording time for one spectrum did not exceed 30 s. The spectra were measured with a temperature step of 0.4 K. The studied samples were optically transparent unoriented single crystals of greenish color less than 3 mm in size with a natural faceting and did not contain defects and inclusions of different colors visible under a microscope. The temperature of the structural phase transition was determined from the temperatures of anomalies in the spectra, including the appearance of new lines in the Raman spectrum, and by analyzing the behavior of soft modes. The transition temperature was corrected considering the sample heating by laser radiation according to the procedure described in the paper [31].

To control the composition of elements of the crystals under study, X-ray energy-dispersive microscopy (XEDM) of the above crystals was carried out at an accelerating voltage of 20 kV on TM4000Plus desktop scanning electron microscope (Hitachi, Japan), combined with XFlash Detector 630Hc energy-dispersive detector (Bruker, Germany), which allows X-ray mapping. Before microscopy the samples were not subjected to any additional processing: thin layers of metal or carbon were not applied on their surface, so as not to introduce additional errors into the experiment. Samples preparation was as follows. The crystal was freshly cleaved, then, using a double-sided carbon conductive tape for XEDM (Ted Pella, Inc., USA), the sample was mounted on a copper substrate, made of anode copper, for XEDM to exclude possible impurities during EDX analysis. Due to the presence of a carbon tape for XEDM, the carbon content on X-ray maps was increased. Since TM4000Plus microscope operates in the mode of back scattered electrons (BSE) detector, the map is presented in phase contrast format, which makes it possible to assess the sample homogeneity in terms of chemical composition: the heavier the element is (the higher the serial number Z is), the brighter it is. An analysis of BSE maps showed that all studied crystals were homogeneous, and no anomalies in the distribution of elements were found.

RESULTS AND DISCUSSION

During structural phase transitions of the second order or transitions of the first order, close to the tricritical point, the frequency of one or more normal modes of the crystal lattice tends to zero or greatly decreases. The lowest frequency mode with anomalous drop is usually called „soft mode“. The concept and theory of the soft mode, as well as the terminology associated with the condensation of soft modes and their subsequent restoration in the distorted phase after a phase transition, was considered in a large number of theoretical and experimental studies. In short article related to spectral studies of phase transitions in huntite crystals, it would be inappropriately to describe the history of this topic. We can only refer to some papers as a good starting point for studying this phenomenon [37, 38]. An excellent review of soft mode spectroscopy at an early stage of such studies was given by Scott [39].

While studying the RS temperature spectra in the series of solid solutions $TbFe_{3-x}Ga_x(BO_3)_4$, our attention was drawn to the unusual behavior of soft modes. Note that soft modes and structural phase transitions in crystals $TbFe_3(BO_3)_4$ and $TbFe_{2.5}Ga_{0.5}(BO_3)_4$ were studied earlier [9, 32]. To get a more complete picture of the phase transitions temperature dependence when iron ions are replaced by gallium ions, we repeated the studies of these two crystals and included two new crystals in the study: $TbFe_{2.45}Ga_{0.55}(BO_3)_4$ and $TbFe_{2.4}Ga_{0.6}(BO_3)_4$.

The behavior of the spectra with temperature change in the low-frequency region is shown in Fig. 1. In $TbFe_3(BO_3)_4$ crystal below the structural phase transition point one soft mode is restored (Fig. 1a) (soft modes are marked with asterisks in the figure). The intensity map (Fig. 2) of $TbFe_3(BO_3)_4$ crystal clearly shows that the intensity of this line decreases almost to zero near the transition, while its frequency does not reach zero. This is explained by the fact that this mode appears due to the folding of the Brillouin zone when the symmetry is lowered from $R32$ to $P3_121$ with a tripling of the unit cell volume and the associated transition of phonon from the acoustic branch to the edge of the zone [9]. A shift in the soft mode frequency is observed below 50 K, which is related to the magnetoelastic interaction between the structural and magnetic order parameters. A similar behavior of the soft mode was previously observed in $HoFe_{2.5}Ga_{0.5}(BO_3)_4$ crystal [40]. The temperature of the structural phase transition, determined from the behavior of the spectral lines in this crystal, is 198 K, which agrees with the results published earlier [9].

In the spectra of $TbFe_{2.5}Ga_{0.5}(BO_3)_4$ crystal (unlike the previous crystal) both condensation and recovery

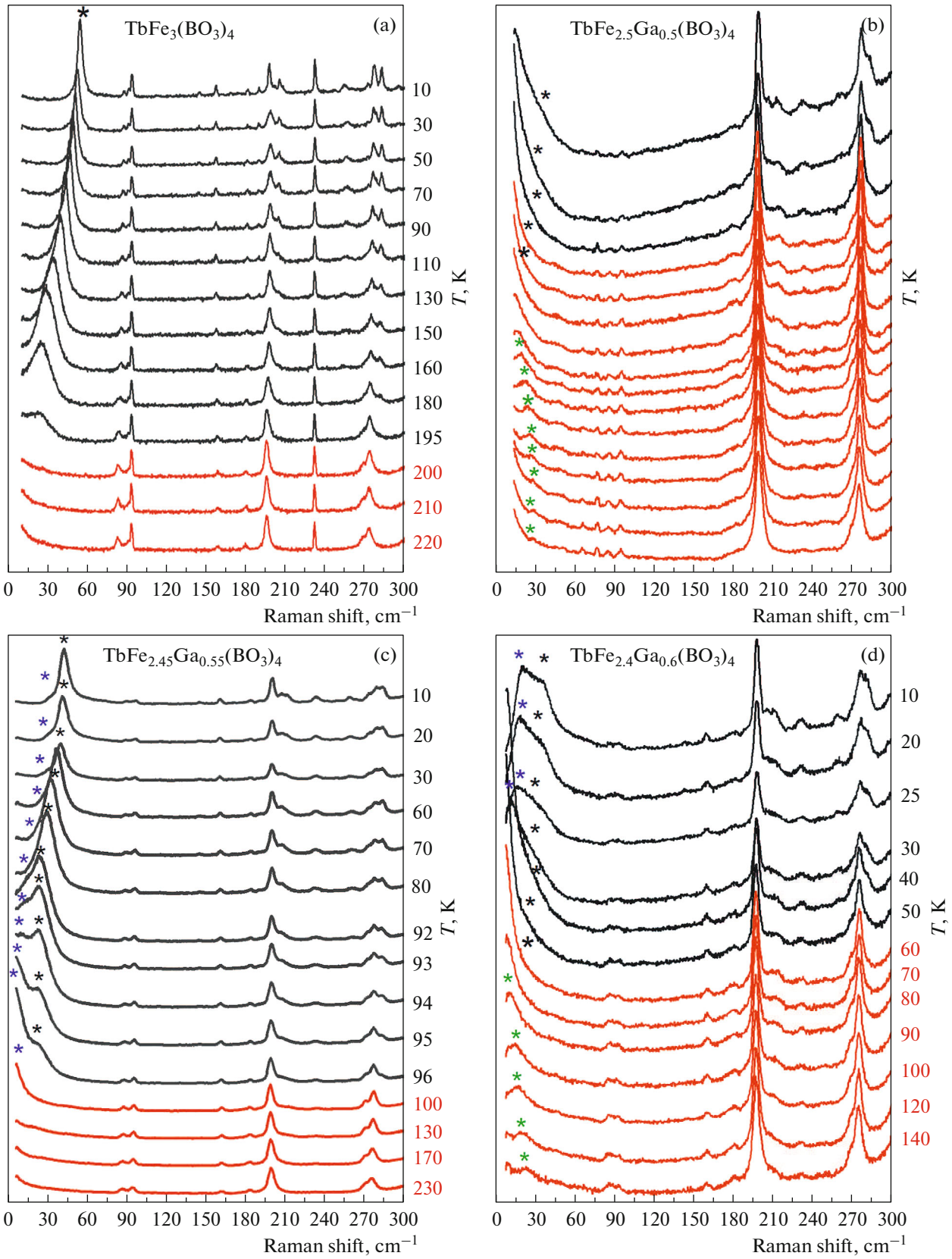

Fig. 1. Temperature transformation of RS spectra in low-frequency range for solid solutions (by embedding): (a) $TbFe_3(BO_3)_4$, (b) $TbFe_{2.5}Ga_{0.5}(BO_3)_4$, (c) $TbFe_{2.45}Ga_{0.55}(BO_3)_4$, (d) $TbFe_{2.55}Ga_{0.45}(BO_3)_4$. Asterisks denote soft modes. The high-temperature phase is in red color, the low-temperature—in black.

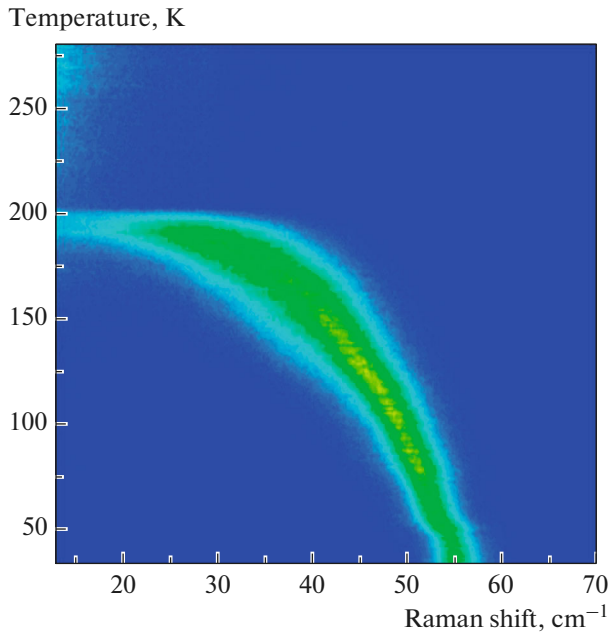

Fig. 2. Intensity map at low frequencies in the crystal $TbFe_3(BO_3)_4$.

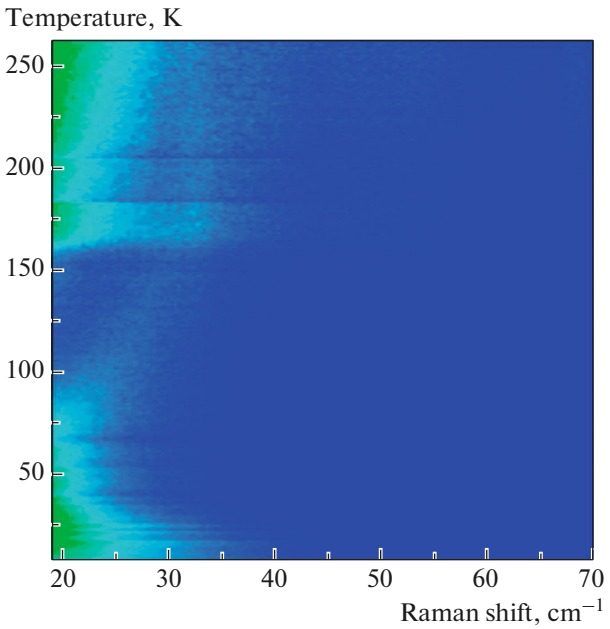

Fig. 3. Intensity map at low frequencies in $TbFe_{2.5}Ga_{0.5}(BO_3)_4$ crystal (by embedding).

of the soft mode are observed (Fig. 1b). The soft mode condenses upon cooling in the highly symmetric phase and then restores upon further cooling below the phase transition from 33 to 10 K.

Usually, due to symmetry limitations, only the soft mode restoration in the low-symmetry phase after the transition is observed in RS spectra. In this case, this behavior can explain both the result of the crystal symmetry violation caused by the strong interaction of the structural order parameter with the magnetic sublattice due to the closeness of the temperatures of the structural and magnetic transitions in the mixed compositions. Such close temperatures of these transitions have not been observed previously in other borates with the huntite structure. Significantly, for a pure composition the soft mode condensation is not observed in the Raman spectrum of the highly symmetric phase, this agrees with the results of the group-theoretic analysis and numerical simulation.

The structural transition temperature in $TbFe_{2.5}Ga_{0.5}(BO_3)_4$ crystal is 33 K [32]. On the intensity map of $TbFe_{2.5}Ga_{0.5}(BO_3)_4$ crystal in addition to soft mode condensation we also observe the restoration of the second soft mode with temperature increasing (Fig. 3).

In solid solution crystal $TbFe_{2.45}Ga_{0.55}(BO_3)_4$ we see the restoration of two close low-frequency modes (Fig. 1c). In this case, the frequency of one mode tends to zero when approaching the phase transition temperature T_c, and the movement of the second mode stops a few degrees before the transition, then its intensity decreases, and at temperature T_c it completely disappears. In this crystal, the structural transition temperature is T_c = 97 K. On the temperature map of the spectral lines intensities of $TbFe_{2.45}Ga_{0.55}(BO_3)_4$ crystal (Fig. 4) the condensation of two closely spaced modes is seen from the increasing of the spectral region occupied by the lines when approaching the transition temperature. The stop of one line motion leads to the appearance of a constriction on the intensity map in the frequency region of 15 cm^{-1}. One can also notice the magnetoelastic interaction influence on the soft mode behavior below 40 K (Fig. 4).

In the spectra of $TbFe_{2.4}Ga_{0.6}(BO_3)_4$ crystal we also observe the condensation of one low-frequency mode as the temperature decreases to the phase transition point and the subsequent restoration of two close modes (Fig. 1d) upon further cooling. Phase transition temperature is T_c = 56 K. On the intensity map of $TbFe_{2.4}Ga_{0.6}(BO_3)_4$ crystal (Fig. 5) one can see a weak peak condensing towards the transition and two close restoring modes upon further cooling of the crystal. X-ray diffraction studies performed on samples from the same crystallization unambiguously indicate the transition from the phase $R32$ to the phase $P3_121$ with temperature decreasing. In general, the behavior of soft modes in this solid solution is similar to that observed in solid solution $TbFe_{2.45}Ga_{0.55}(BO_3)_4$.The structural phase transition from the phase $R32$ to the phase $P3_121$ in $TbFe_3(BO_3)_4$ crystal, according to the calculation, is associated with the phonon mode condensation at the point of the Brillouin zone, followed

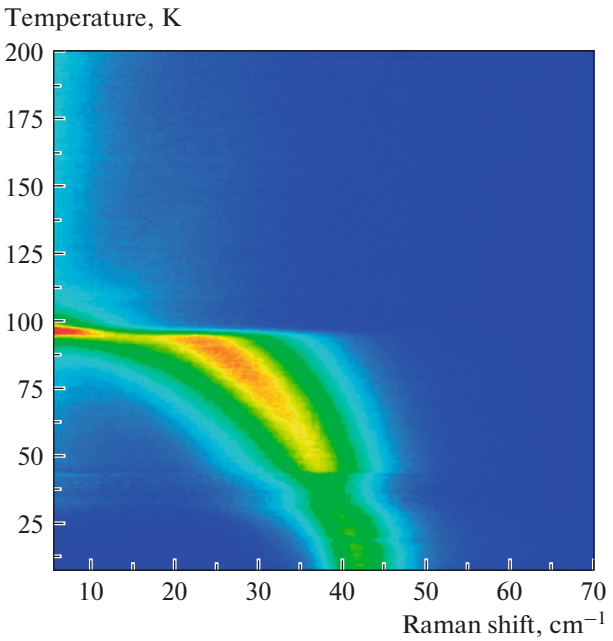

Fig. 4. Intensity map at low frequencies in $TbFe_{2.45}Ga_{0.55}(BO_3)_4$ crystal (by embedding).

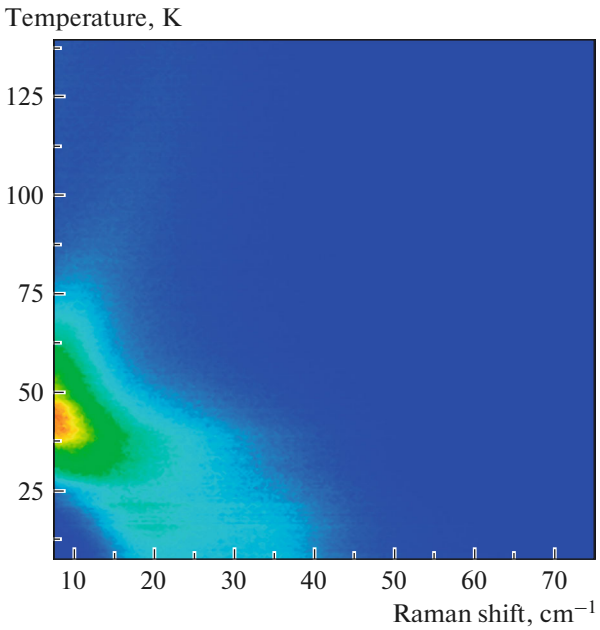

Fig. 5. Intensity map at low frequencies in $TbFe_{2.4}Ga_{0.6}(BO_3)_4$ crystal (by embedding). The structural transition temperature (56 K) is presumably close to the magnetic transition temperature (not yet determined) of the solid solution.

by zone "folding." As a result, phonons from the point Λ of the high-temperature phase end at the point Γ of the Brillouin zone of the low-temperature phase [15]. Experimentally, in Raman spectra of crystals with mixed compositions we observe two low-frequency modes: before and after the transition. Such behavior is possible if we observe soft mode from the point Λ of the Brillouin zone of the high-temperature phase due to violation of the selection rules, which is probably caused by strong interaction with the magnetic sublattice due to the closeness of the temperatures of the structural and magnetic transitions and the disorder of the lattices of the mixed crystals.

When considering a separate spectrum at one particular temperature, it is practically impossible to notice on Raman spectrum the line corresponding to the "soft" mode in the phase *R*32, however, its temperature behavior and motion can be very clearly seen in the sequential animation of temperature spectra and temperature maps of intensity scattering. The very weak signal of this mode does not allow to decompose the contour with the subsequent presentation of the line position or its parameters versus temperature.

The analysis of the dependence of the temperatures of structural phase transitions on the composition showed the absence of a monotonic dependence between the embedding of gallium during the synthesis of solid solutions and the temperature of phase transitions. The behavior of soft mode frequencies also does not correlate with the concentration of gallium in the embeddings. To clarify the question of the existence of the transition temperatures dependence on the gallium content in crystals, the compositions of solid solutions were refined.

Additionally, studies were carried out by X-ray energy-dispersive microscopy, and the gallium content in all the crystals studied in the work was determined from its results. The results of refinement of the

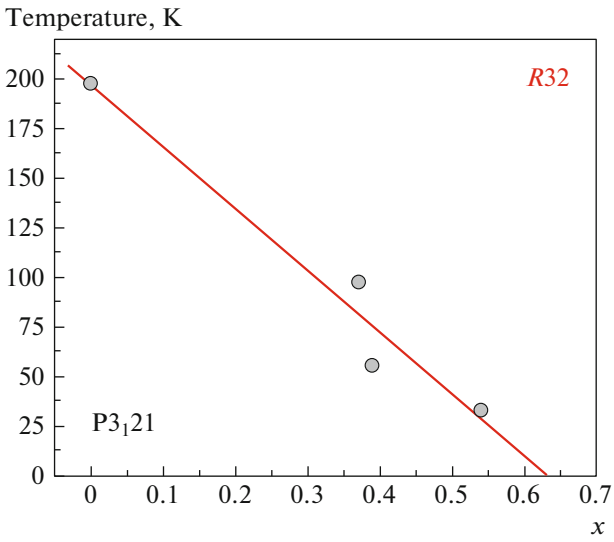

Fig. 6. Phase diagram: temperature of structural transition in solid solutions $TbFe_{3-x}Ga_x(BO_3)_4$ vs gallium content.

Table 2. Refinement of gallium content in solid solutions $TbFe_{3-x}Ga_x(BO_3)_4$ and structural transition temperatures

Formula by embedding during growth	Formula by XEDM result	T, K
$TbFe_3(BO_3)_4$	$TbFe_3(BO_3)_4$	198
$TbFe_{2.5}Ga_{0.5}(BO_3)_4$	$TbFe_{2.46}Ga_{0.54}(BO_3)_4$	33
$TbFe_{2.45}Ga_{0.55}(BO_3)_4$	$TbFe_{2.63}Ga_{0.37}(BO_3)_4$	97
$TbFe_{2.4}Ga_{0.6}(BO_3)_4$	$TbFe_{2.61}Ga_{0.39}(BO_3)_4$	56

concentrations of iron and gallium ions in the composition of solid solutions are presented in the Table 2. The phase diagram "Composition-Temperature" (Fig. 6) was prepared using the refined data and the phase transition temperatures determined earlier. The error in determining the phase boundary (on the basis of the obtained data) was 9%. Besides, XEDM analysis showed that in samples $TbFe_{2.46}Ga_{0.54}(BO_3)_4$ and $TbFe_{2.4}Ga_{0.6}(BO_3)_4$ a small inclusions of Bi atoms were found in the composition, while in later synthesized crystals with the compositions $TbFe_{2.46}Ga_{0.54}(BO_3)_4$ and $TbFe_{2.4}Ga_{0.6}(BO_3)_4$ no Bi atoms were found to be included in the composition.

Changes in the composition of solid crystals slightly affect the temperature change of the structure magnetic ordering, which for the studied compositions lies in the range of 35–50 K. Approximately, the magnetic ordering temperatures can also be determined from the anomalies in the RS spectra in the high-frequency range. According to these data, at the concentration of Ga atoms in the composition at a level of $x = 0.5$–0.6, it is possible to obtain crystals of solid solutions, in which the temperatures of the structural and magnetic transitions will be very close or coincide. This can lead to a very strong interaction between the structural and magnetic order parameters (close in temperature soft modes). Such crystals can become good model objects for studying magnetoelastic interactions in multiferroics.

CONCLUSION

In the present work, single crystals of solid solutions $TbFe_{3-x}Ga_x(BO_3)_4$ ($x = 0$, 0.54, 0.39, 0.37) were synthesized. The concentration of Fe and Ga ions in the synthesized solid solution crystals was refined by XEDM. Temperature studies of single crystals of solid solutions were performed by RS spectroscopy. In all the studied samples $TbFe_3(BO_3)_4$, $TbFe_{2.46}Ga_{0.54}(BO_3)_4$, $TbFe_{2.61}Ga_{0.39}(BO_3)_4$, $TbFe_{2.63}Ga_{0.37}(BO_3)_4$ spectral anomalies were observed, which are characteristic for the soft modes restoration in the low-symmetry phase. It is found that in the presence and with an increasing of the substitution of Fe ions by Ga ions in crystals $TbFe_{2.63}Ga_{0.37}(BO_3)_4$, $TbFe_{2.61}Ga_{0.39}(BO_3)_4$ and $TbFe_{2.46}Ga_{0.54}(BO_3)_4$, one more restoring low-frequency mode becomes visible in the spectra, as well as in the highly symmetric phase $R32$ the low-frequency mode is activated, which condenses when the crystal is cooled to the point of the structural phase transition. A significant effect of the iron ions substitution by gallium ions in solid solutions $TbFe_{3-x}Ga_x(BO_3)_4$ on the temperature of the structural phase transition was observed. The increasing of Ga ions concentration in solid solutions leads to the decreasing of the structural transition temperature from the phase $R32$ to the phase $P3_121$; in $TbFe_{2\cdot46}Ga_{0\cdot54}(BO_3)_4$ crystal the temperatures of the structural transition and the transition of magnetic ordering practically coincide. The temperature dependences of the restoring low-frequency modes exhibit small anomalies associated with the interaction of the magnetoelastic and structural order parameters.

ACKNOWLEDGMENTS

During the studies the equipment of the Krasnoyarsk Regional Center for Collective Use of the FRC KSC of the Siberian Branch of the Russian Academy of Sciences was used.

FUNDING

The authors are grateful to the Russian Foundation for Basic Research, the Government of the Krasnoyarsk Territory and the Krasnoyarsk Regional Science Foundation for funding within the framework of the scientific project, grant no. 20-42-240009 r_a_Krasnoyarsk, as well as the Russian Foundation for Basic Research and the German Scientific Research Community (Deutsche Forschungsgemeinschaft) for financial support within the project no. 21-52-12018 NNIO_a.

CONFLICT OF INTEREST

The authors of this work declare that they have no conflict of interest.

REFERENCES

1. G. M. Kuz'micheva, I. A. Kaurova, V. B. Rybakov, V. V. Podbel'skiy, Crystals, **9**. P. 100 (2019). https://doi.org/10.3390/cryst9020100
2. M. Fiebig. J. Phys. D.: Appl. Phys., **38**, R123 (2005). https://doi.org/10.1088/0022-3727/38/8/R01
3. A. M. Kadomtseva, Yu. F. Popov, G. P. Vorob'ev, A. P. Pyatakov, S. S. Krotov, K. I. Kamilov, V. Yu. Ivanov, A.A. Mukhin, K. Zvezdin, A. M. Kuz'menko, L.N. Bezmaternykh, A. Gudim, V. L. Temerov, Low Temperature Physics, **36**, 511 (2010). https://doi.org/10.1063/1.3457390

4. A. N. Vasiliev, E. A. Popova, Low Temperature Physics, **32**, 735 (2006). https://doi.org/10.1063/1.2219496

5. W. Eerenstein, N. D. Mathur, J. F. Scott, Nature, **442**, 759 (2006). https://doi.org/10.103 8/nature05023

6. M. M. Vopson, Critical Reviews in Solid State and Materials Sciences, **40** (4), 223 (2015). https://doi.org/10.1080/10408436.2014.992584

7. N. I. Leonyuk, L. I. Leonyuk, Prog. Crystal Growth. and Charact., **31**, 179 (1995).

8. L. Bezmaternykh, V. Temerov, I. Gudim, N. Stolbovaya, Crystallography Reports, **50**, s97 (2005). https://doi.org/10.1134/1.2133981

9. D. Fausti, A. A. Nugroho, P.H.M. van Loosdrecht, S. A. Klimin, M. N. Popova, L. N. Bezmaternykh, Phys. Rev. B, **74**, 024403 (2006). https://doi.org/10.1103/PhysRevB.74.024403

10. C. Ritter, A. Balaev, A. Vorotynov, G. Petrakovskii, D. Velikanov, V. Temerov, I. Gudim, J. Phys.: Condens. Matters, **19**, 196227 (2007). https://doi.org/10.1088/0953-8984/19/19/196227

11. V. V. Kurnosov, V. S. Tsapenko, L. N. Bezmaternykh, I. A. Gudim, Low Temperature Physics, **40** (12), 1087 (2014). https://doi.org/10.1063/1.4904002

12. Y. Hinatsu, Y. Doi, K. Ito, M. Wakeshima, A. Alemi, J. Solid State Chem., **172**, 438 (2003). https://doi.org/10.1016/S0022- 4596(03)00028-8

13. E. Moshkina, S. Krylova, I. Gudim, M. Molokeev, V. Temerov, M. Pavlovskiy, A. Vtyurin, A. Krylov, Cryst. Growth Des., **20**, 1058 (2020). https://doi.org/10.1021/acs.cgd.9b01387

14. E. A. Popova, D. V. Volkov, A. N. Vasiliev, A. A. Demidov, N. P. Kolmakova, I. A. Gudim, L. N. Bezmatenykh, N. Tristan, Yu. Skourski, B. Buchner, C. Hess, R. Klingeler, Phys. Rev. B, **75**, 224413 (2007). https://doi.org/10.1103/PhysRevB.75.224413

15. M. S. Pavlovskiy, K. A. Shaykhutdinov, L. S. Wu, G. Ehlers, V. L. Temerov, I. A. Gudim, A. S. Shinkorenko, A. Podlesnyak, Phys. Rev. B, **97**, 054313 (2018) https://doi.org/10.1103/Phys- RevB.97.054313

16. D. V. Volkov, E. A. Popova, N. P. Kolmakov, A. A. Demidov, N. Tristan, Yu. Skourski, B. Buechner, I. A. Gudim, L. N. Bezmaternykh, J. Magn. Magn. Mater., **316**, e717 (2007). https://doi.org/10.1016/j.jmmm.2007.03.070

17. T. N. Stanislavchuk, E. P. Chukalina, L. N. Bezmaternykh, J. Opt. Technol., **74**, 130 (2007). https://doi.org/10.1364/JOT.74.000139

18. U. Adem, L. Wang, D. Fausti, W. Schottenhamel, P.H.M. van Loosdrecht, A. Vasiliev, L. N. Bezmaternykh, Buchner, C. Hess, R. Klingeler, Phys. Rev. B, **82**, 064406 (2010). https://doi.org/10.1103/PhysRevB.82.064406

19. A. V. Malakhovskii, S. L. Gnatchenko, I. S. Kachur, V. G. Piryatinskaya, A. L. Sukhachev, V. L. Temerov, Eur. Phys. J. B, **80**, 1 (2011). https://doi.org/10.1140/epjb/e2011-10806-x

20. M. N. Popova, T. N. Stanislavchuk, B. Z. Malkin, L. N. Bezmaternykh, J. Phys.: Condens. Matter, **24** (19), 196002 (2012). https://doi.org/10.1088/0953-8984/24/19/196002

21. S. L. Gnatchenko, I. S. Kachur, V. G. Piryatinskaya, V. A. Bedarev, M. I. Pashchenko, Low Temp. Phys., **37**, 693 (2011). https://doi.org/10.1063/1.3660219

22. D. Szaller, V. Kocsis, S. Bordacs, T. Feher, T. Room, U. Nagel, H. Engelkamp, K. Ohgushi, I. Kezsmarki, Phys. Rev. B, **95**, 024427 (2017). https://doi.org/10.1103/PhysRevB.95.024427

23. S. Krylova, I. Gudim, A. Aleksandrovsky, A. Vtyurin, A. Krylov, Ferroelectrics, **575** (1), 11 (2021). https://doi.org/10.1080/00150193.2021.1888219

24. S. N. Krylova, A. S. Aleksandrovsky, E. M. Roginskii, A. A. Krylov, I. A. Gudim, A. N. Vtyurin, Ferroelectrics, **559** (1), 135 (2020). https://doi.org/10.1080/00150193.2020.1722015

25. R. Z. Levitin, E. A. Popova, R. M. Chtsherbov, A. N. Vasiliev, M. N. Popova, E. P. Chukalina, S. A. Klimin, P. H. M. van Loosdrecht, D. Fausti, L. N. Bezmaternykh, JETP Lett., **79**, 423 . https://doi.org/10.1134/1.1776236

26. S. A. Klimin, D. Fausti, A. Meetsma, L. N. Bezmaternykh, P.H.M. van Loosdrechta, T. T. Palstra, Acta Cryst. B, **61**, 481 . https://doi.org/10.1107/S0108768105017362

27. A. S. Krylov, I. A. Gudim, I. Nemtsev, S. N. Krylova, A. V. Shabanov, A. A. Krylov, J. Raman Spectrosc., **48**, 1406 (2017). https://doi.org/10.1002/jrs.5078

28. E. Moshkina, A. Krylov, S. Sofronova, I. Gudim, V. Temerov, Cryst. Growth Des., **16**, 6915 (2016). https://doi.org/10.1021/acs.cgd.6b01079

29. E. Moshkina, I. Gudim, V. Temerov, A. Krylov, J. Raman Spectrosc., **49**, 1732 (2018). https://doi.org/10.1002/jrs.5430

30. A. S. Krylov, S. N. Sofronova, I. A. Gudim, A. N. Vtyurin, Solid State Commun., **174**, 26 (2013). https://doi.org/10.1016/j.ssc.2013.09.011

31. A. S. Krylov, S. N. Sofronova, I. A. Gudim, S. N. Krylova, R. Kumar, A. N. Vtyurin, J. Adv. Dielectr., **8**, 1850011 (2018). https://doi.org/10.1142/S2010135X1850011X

32. A. S. Krylov, I. A. Gudim, S. N. Krylova, A. A. Krylov, A. N. Vtyurin, Ferroelectrics, **559**, 128 (2020). https://doi.org/10.1080/00150193.2020.1722014

33. A. V. Peschanskii, A. V. Yeremenko, V. I. Fomin, L. N. Bezmaternykh, I. A. Gudim, Low Temperature Physics, **40**, 171 (2014). https://doi.org/10.1063/1.4865566 17

34. S. A. Klimin, A. B. Kuzmenko, M. A. Kashchenko, M. N. Popova, Phys. Rev. B, **93**, 054304 (2016). https://doi.org/10.1103/PhysRevB.93.054304

35. M. N. Popova, J. Magn. Magn. Mat., **321** (7), 716 (2009). https://doi.org/10.1016/j.jmmm.2008.11.033

36. L. N. Bezmaternykh, S. A. Kharlamova, V. L. Temerov, Kristal lografiya, **49** (4), 1 (2004) (in Russian).

37. V. L. Ginzburg, Ferroelectrics, **76** (1), 3 (1987). https://doi.org/10.1080/00150198708009019

38. L. D. Landau, E. M. Lifshitz, Statistical physics. Part 1 (Pergamon Press, Oxford, 1980).

39. J. F. Scott, Rev. Mod. Phys. **46** (1), 83 (1974). https://doi.org/10.1103/RevModPhys.46.83

40. A. Krylov, S. Krylova, I. Gudim, A. Vtyurin, Ferroelectrics, **556**, 16 (2020). https://doi.org/10.1080/00150193.2020.1713334